GEOPHYSICAL RESEARCH LETTERS, VOL. 35, L20401, doi:10.1029/2008GL034150, 2008

Estimation of bathymetric depth and slope from data assimilation of swath altimetry into a hydrodynamic model

Michael Durand,[1] Konstantinos M. Andreadis,[2] Douglas E. Alsdorf,[1,3] Dennis P. Lettenmaier,[2] Delwyn Moller,[4] and Matthew Wilson[5]

Received 27 March 2008; revised 29 May 2008; accepted 8 August 2008; published 17 October 2008.

[1] The proposed Surface Water and Ocean Topography (SWOT) mission would provide measurements of water surface elevation (WSE) for characterization of storage change and discharge. River channel bathymetry is a significant source of uncertainty in estimating discharge from WSE measurements, however. In this paper, we demonstrate an ensemble-based data assimilation (DA) methodology for estimating bathymetric depth and slope from WSE measurements and the LISFLOOD-FP hydrodynamic model. We performed two proof-of-concept experiments using synthetically generated SWOT measurements. The experiments demonstrated that bathymetric depth and slope can be estimated to within 3.0 microradians or 50 cm, respectively, using SWOT WSE measurements, within the context of our DA and modeling framework. We found that channel bathymetry estimation accuracy is relatively insensitive to SWOT measurement error, because uncertainty in LISFLOOD-FP inputs (such as channel roughness and upstream boundary conditions) is likely to be of greater magnitude than measurement error.
Citation: Durand, M., K. M. Andreadis, D. E. Alsdorf, D. P. Lettenmaier, D. Moller, and M. Wilson (2008), Estimation of bathymetric depth and slope from data assimilation of swath altimetry into a hydrodynamic model, *Geophys. Res. Lett.*, *35*, L20401, doi:10.1029/2008GL034150.

1. Introduction

[2] The spatial distribution and temporal dynamics of surface water storage, as well as the discharge of streams and rivers, are significant components of the global water balance [*Oki and Kanae*, 2006]. Current spaceborne remote sensing techniques demonstrate great potential for characterization of surface water, including inundated area [*Smith*, 1997], the gravity field of water storage changes via GRACE [e.g., *Rodell and Famiglietti*, 2001; *Han et al.*, 2005], and surface water elevations via altimetry [e.g., *Frappart et al.*, 2006]. However, *Alsdorf et al.* [2007] noted that none of the existing remote sensing methods alone is adequate to provide needed constraints on the global water cycle. Limitations include poor spatial resolution from the GRACE mission or point-based measurements from altimetry. The Surface Water and Ocean Topography (SWOT) mission is a swath mapping radar altimeter that would provide new measurements of inland water surface elevation (WSE) for rivers, lakes, wetlands and reservoirs. SWOT has been recommended by the National Research Council (NRC) Decadal Survey [*National Research Council*, 2007] to measure ocean topography as well as WSE over land; the proposed launch date timeframe is between 2013–2016.

[3] While calculation of water elevations and storage changes will be straightforward from SWOT WSE measurements, discharge estimation is more difficult because it requires key first-order hydraulic parameters, such as channel bathymetry and Manning's roughness coefficient, which are not directly measurable from space. Data assimilation (DA) represents an opportunity to overcome these limitations. For example, *Andreadis et al.* [2007] have demonstrated the assimilation of SWOT measurements into the LISFLOOD-FP [*Bates and De Roo*, 2000] raster-based hydrodynamic model in order to characterize discharge for a reach of the Ohio River. While *Andreadis et al.* [2007] updated the LISFLOOD-FP model states, the purpose of this paper is to illustrate the estimation of (time-invariant) bathymetric depth and slope, using synthetically-generated SWOT measurements and a DA methodology. We also examine the sensitivity of the bathymetric depth estimates to SWOT measurement errors.

2. Methods

2.1. Study Area

[4] The dynamics of seasonally flooded wetlands in the Amazon basin control a variety of ecologically-important processes, including plant productivity [*Wittman et al.*, 2004] and nutrient dynamics [*Melack and Forsberg*, 2001]. Recent modeling [e.g., *Coe et al.*, 2002; *Alsdorf et al.*, 2005; *Wilson et al.*, 2007] and remote sensing [e.g., *Hamilton et al.*, 2002; *Alsdorf et al.*, 2007] studies, have improved our understanding of Amazon hydraulic processes such that our SWOT virtual mission hydrodynamic model is sufficiently representative of reality. In this study, our domain is a 240 km reach of the Amazon River modeled by *Wilson et al.* [2007]; see Figure 1.

2.2. LISFLOOD-FP Hydrodynamics Model

[5] LISFLOOD-FP is a raster-based model designed to characterize floodplain dynamics over complex topography [*Bates and De Roo*, 2000]. Inputs include floodplain DEM, bathymetric depths, channel widths, channel roughness, and

[1]Byrd Polar Research Center, Ohio State University, Columbus, Ohio, USA.
[2]Department of Civil and Environmental Engineering, University of Washington, Seattle, Washington, USA.
[3]Also at Department of Earth Sciences, Ohio State University, Columbus, Ohio, USA.
[4]NASA Jet Propulsion Laboratory, Pasadena, California, USA.
[5]University of the West Indies, St. Augustine, Trinidad and Tobago.

0094-8276/08/2008GL034150$05.00

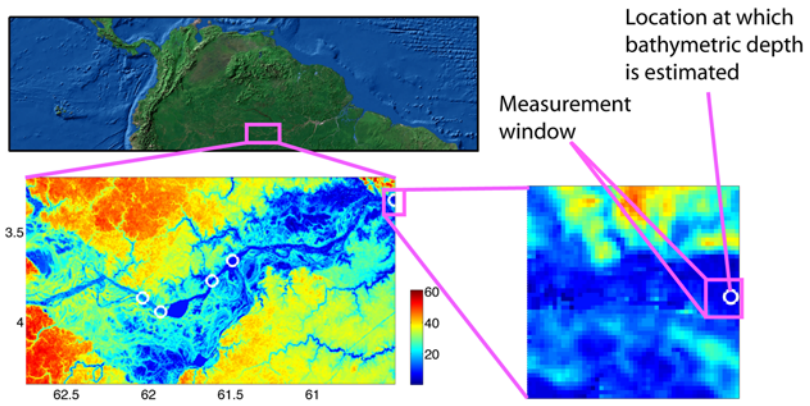

Figure 1. (bottom left) The study area DEM in (top) the Amazon River basin is shown. The white circles are the locations at which channel depth is estimated. (bottom right) Channel depth is estimated using SWOT floodplain WSE measurements in the measurement window, illustrated for the far downstream location.

upstream flow boundary conditions. In this study, we utilize the LISFLOOD nominal inputs described by *Wilson et al.* [2007]. We model uncertainty for input variables by 1) making assumptions about the probability distribution function and 2) using Monte Carlo methods to generate an ensemble of each input, as follows. Bathymetric slope uncertainty is modeled with mean unity multiplicative log-normal error (MLNE) with a coefficient of variation of 0.47, resulting in a reasonable range of slopes in the ensemble, from 1.5 to 6.0 cm km^{-1}. The slope was used to calculate the bathymetric depths to use to drive LISFLOOD. Uncertainty in channel roughness was modeled with mean unity MLNE with coefficient of variation of 0.06, resulting in a range of channel roughness from 0.0214 to 0.0276, corresponding with the uncertainty estimate of *Wilson et al.* [2007]. Uncertainty in upstream flow boundary conditions was modeled with mean unity MLNE with coefficient of variation of 0.06, corresponding with the uncertainty in estimating flow from a stage-rating curve [e.g., *Dingman*, 2000]. Uncertainty in the 270 m floodplain DEM is modeled with mean zero additive normal error with standard deviation of 2.0 meters, corresponding with the uncertainty estimate of *Wilson et al.* [2007].

2.3. Synthetic SWOT Measurements

[6] As described by *Alsdorf et al.* [2007], the technology for SWOT is a Ka Band Radar Interferometer (KaRIN) with a swath width of 120 km. Random and systematic measurement errors derive from several sources, including thermal noise, spatio-temporal variability in path delay due to atmospheric water vapor, and layover due to topography and vegetation [*Rodríguez and Moller*, 2004; *Alsdorf et al.*, 2007]. WSE measurements and inundated area classification can be obtained from the radar signal. One goal of this paper is to examine the sensitivity of the DA estimates of bathymetric depth to the magnitude of SWOT measurement errors. We represent SWOT measurements z_{obs} as the true WSE plus measurement error v. We use a LISFLOOD-FP simulation to obtain the true WSE, and assume that v follows a normal distribution with mean μ_v and standard deviation σ_v. We investigate sensitivity of the DA methodology to random and systematic errors by varying σ_v and μ_v, respectively, for an arbitrary range up to 50 cm for the WSE measurements, which should encompass the range of error characteristics for the real instrument. Inundated area measurements errors are assumed to be unbiased with a standard deviation of 2.5 %.

2.4. Data Assimilation

[7] The estimation of channel bathymetry amounts to the estimation of model parameters without directly estimating the model state variables. Here, we extend the linear parameter estimator of *Balakrishnan* [2005] to the non-linear case using Monte Carlo techniques, following *Evensen* [1994]. The prior ensemble (see section 2.2) stochastically characterizes the relationship between WSE, channel bathymetry, and other model inputs. The posterior estimate of bathymetry (either bathymetric depth or bathymetric slope, see section 2.5) can be derived from statistics calculated across the prior ensemble in analysis similar to the EnKF update [*Evensen*, 1994]:

$$\alpha_k^+ = \alpha_k^- + C_{\alpha z}(C_{zz} + \Lambda_v)^{-1}(z_{obs} + w_k - z_{pred,k}) \qquad (1)$$

where α_k^- and α_k^+ are the prior and posterior bathymetry estimates, respectively, for each replicate $k = 1,2,\ldots n_k$, where n_k is the ensemble size; w_k is a randomly-generated mean zero normal variable with standard deviation of σ_v, and is a necessary correction to *Evensen* [1994], as explained by *Burgers et al.* [1998]. In this study, we use an ensemble size n_k of 20, following *Andreadis et al.* [2007]. The vectors z_{obs} and $z_{pred,k}$ are the observed and predicted timeseries, respectively, of either WSE or inundated area, with length n_m. The matrices $C_{\alpha z}$ and C_{zz} are the covariance matrix of the bathymetry estimates with the predicted measurements, and the covariance matrix of the predicted measurements, respectively; both are calculated directly from the ensemble. The matrix Λ_v is the assumed error covariance of the WSE measurements, calculated as the product of the scalar σ_v^2 and the n_m-dimensional identity matrix; thus, we assume that measurement error variance is constant in space and time, which is valid as a first-order approximation. Provided the posterior estimate of bathymetry, a retrospective posterior estimate of

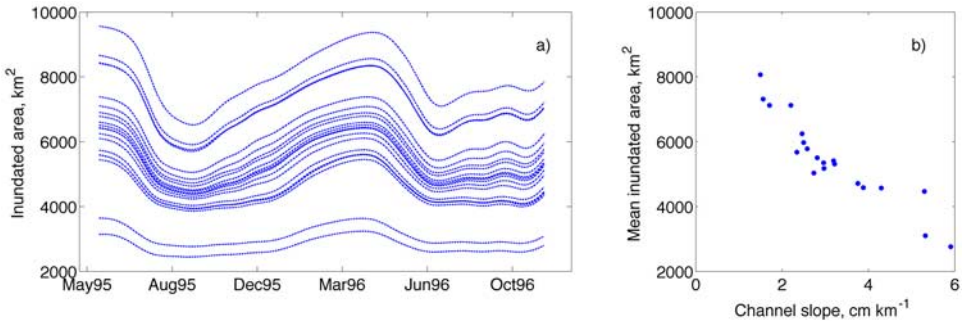

Figure 2. (a) Inundated area output from the LISFLOOD-FP model is shown for the 22-month study period for the ensemble of model runs. (b) The relationship between the bathymetric slope and temporal mean inundated area is also shown.

the WSE and discharge can easily be obtained via forward model simulation.

2.5. Experimental Design

[8] Our objective is to illustrate the utility of SWOT WSE measurements for characterizing channel bathymetry, and to investigate the sensitivity of the bathymetry estimates to SWOT measurement error. We perform two experiments: one in which we estimate average bathymetric slope across the entire domain, and one in which we estimate the bathymetric depth at five locations along the river. In the second experiment, we use a localized spatial subset of the domain to update the bathymetric depth, as illustrated in Figure 1. We chose a spatial subset size ("measurement window" as labeled in Figure 1) of twenty-five 270 m LISFLOOD-FP pixels to be of the same order of magnitude as the spatial correlation length [*Isaaks and Srivastava*, 1989] of the LISFLOOD-FP floodplain WSE model output. For both experiments, The spatial and temporal sampling of LISFLOOD-FP pixels by SWOT was performed by assuming a 16-day Terra-like orbit and the swath coverage described in section 2.2. We represent the ensemble estimates as the mean across the ensemble for both the prior and posterior estimates. We use the LISFLOOD-FP model configuration described by *Wilson et al.* [2007]; the study period is 1 June 1995–31 March 1997.

3. Results and Discussion

3.1. Estimating Bathymetric Depth and Slope

[9] The LISFLOOD-FP model was integrated for each ensemble member; ensemble output is shown in Figure 2. In the first experiment, bathymetric slope was estimated using the ensemble of LISFLOOD-FP model runs and equation (1), where the measurements were the inundated area timeseries. The prior and posterior ensembles of bathymetric slope are

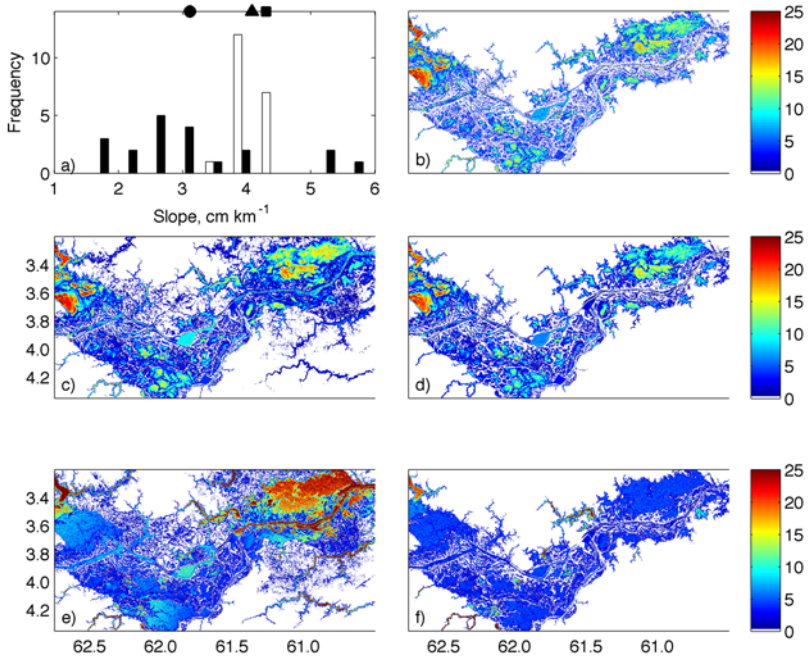

Figure 3. (a) The white and black bars show histograms of the prior and posterior bathymetric slope ensembles, respectively; the true slope (square) and the prior (circle) and posterior (triangle) ensemble mean are also indicated. For 18 September 1995, (b) true WSE, (c) prior and (d) posterior ensemble mean WSE, and (e) prior and (f) posterior ensemble standard deviation are shown.

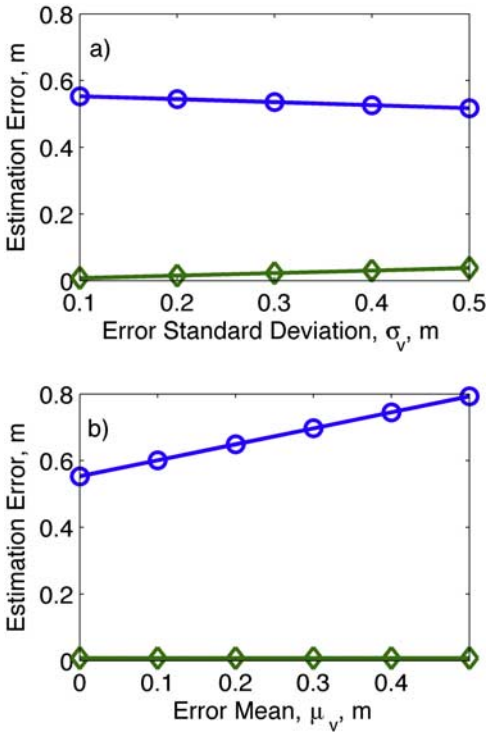

Figure 4. Estimated (diamonds) and actual (circles) channel elevation estimation error are shown (a) as a function of measurement error standard deviation σ_v for fixed error mean μ_v and (b) as a function of μ_v for fixed σ_v.

shown in Figure 3a. The true slope was 4.30 cm km^{-1}, and the prior and posterior slope estimates were 3.1 and 4.08 cm km^{-1}, respectively. The slope was thus estimated to within 0.30 cm km^{-1} (3.0 microradians) of the truth. The prior and posterior ensemble standard deviations were 1.22 and 0.21 cm km^{-1}, respectively. The uncertainty of the posterior estimate approximates (to first order) the error in the posterior estimate. In the second experiment, bathymetric depth at the five nodes shown in Figure 1 was estimated using the ensemble of LISFLOOD-FP model runs and equation (1), where the measurements were WSE, as described in section 2.5. The prior estimate was −4.0 meters, the truth was −7.4 meters, and the posterior estimate was −7.96 meters. The absolute error for the posterior was 0.56 meters, which is 84 % less than the prior absolute error.

[10] We repeated the LISFLOOD-FP model integrations for the posterior ensemble of bathymetric depth obtained during the second experiment. Figure 3b shows the true WSE, and Figures 3c and 3d show the prior and posterior WSE estimates on 18 September, 1995. From inspection, the posterior WSE estimate was similar to the truth, while the prior estimate overestimated WSE. The spatial mean error for the prior and posterior estimates shown was 0.55 meters and −0.19 meters, respectively. The absolute value of the posterior mean error was 65 % less than the absolute value of the prior mean error. The posterior bathymetric depth estimates utilizing SWOT measurements thus effectively corrected the LISFLOOD-FP simulations by correcting the bathymetry inputs. The ensemble standard deviation of the WSE model output provides an estimate of the uncertainty in the LISFLOOD-FP WSE prediction. The prior and posterior WSE standard deviation is shown in Figures 3e and 3f, respectively. The spatial mean standard deviation for the prior and posterior results estimates was 3.97 m and 1.30 meters, respectively. The posterior uncertainty was thus 67 % less than prior uncertainty.

3.2. Estimating Sensitivity to Measurement Error

[11] Figure 4a shows the sensitivity of the predicted error σ_α (i.e., the uncertainty or the ensemble standard deviation of the posterior estimate of bathymetric depth) and the actual error ε_α (i.e., the true bathymetric depth subtracted from the ensemble mean of the posterior estimate of bathymetric depth) for the downstream boundary bathymetric depth to measurement error standard deviation, σ_v, assuming that μ_v is equal to zero. Both σ_α and ε_α are insensitive to σ_v, and σ_α is much less than ε_α. Figure 4b shows the sensitivity of σ_α and ε_α to measurement error bias, μ_v, assuming that σ_v is 0.05 m. Larger values of μ_v are associated with larger values of ε_α, and σ_α is insensitive to μ_v. The lack of sensitivity of the error metrics to σ_v implies that the model error is much larger than the measurement error; thus, the DA analysis gives more weight to measurement than to the model in equation (1). The fact that σ_α is less than ε_α is likely due to the fact that the true model inputs (including channel roughness and upstream boundary conditions) are significantly different than those of the ensemble mean. This results points to a potential limitation of our method; when the model error is much greater than the measurement error, it is possible for the DA analysis to underestimate the posterior parameter uncertainty. The sensitivity of ε_α to μ_v indicates that in the unlikely case of WSE measurements with persistent spatiotemporal biases greater than 10 cm, the posterior bathymetry accuracy is sensitive to both model error and measurement error.

4. Conclusions

[12] In this paper, we have illustrated a new approach to characterize river channel bathymetry using synthetic WSE measurements within the context of a virtual SWOT mission. An ensemble DA methodology was utilized, in which LISFLOOD-FP model runs were used to relate the bathymetry and the WSE observations. Our estimate predicts the first two statistical moments of the bathymetric quantities; i.e., an estimate of the uncertainty or predicted error is obtained in addition to an estimate of the mean or expected value of the bathymetric quantity, conditioned on the observations. We performed two separate proof-of-concept experiments. In the first experiment, we estimated bathymetric slope using inundated area measured over the entire 240 km reach. The slope was estimated to within 0.30 cm km^{-1} (3.0 microradians) of the truth. In the second experiment, we estimated bathymetric depth elevations at five points on the main-stem Amazon River from synthetic WSE measurements. The absolute error for the downstream outlet bathymetric depth was 0.56 meters, which is 84 % less than the prior absolute error. The experiments demonstrated that bathymetry can be accurately estimated using SWOT WSE measurements for the design parameters of the satellite, and that model error will likely dominate over measurement

error, so that estimates of channel bathymetry will be relatively insensitive to measurement error characteristics.

[13] **Acknowledgments.** This work was funded by NASA's Terrestrial Hydrology Program, and by The Ohio State University Climate Water Carbon program (http://bprc.osu.edu/dev/cwc/). We gratefully acknowledge Paul Bates for use of the LISFLOOD-FP model, the computing resources provided by the Ohio Supercomputer Center (OSC; www.osc.edu), and Judy Gardiner of the OSC for help in parallelizing LISFLOOD-FP. Ernesto Rodriguez and two anonymous reviewers provided valuable input that improved the quality of the manuscript.

References

Alsdorf, D. E., T. Dunne, J. Melack, L. Smith, and L. Hess (2005), Diffusion modeling of recessional flow on central Amazonian floodplain, *Geophys. Res. Lett.*, *32*, L21405, doi:10.1029/2005GL024412.

Alsdorf, D. E., E. Rodríguez, and D. P. Lettenmaier (2007), Measuring surface water from space, *Rev. Geophys.*, *45*, RG2002, doi:10.1029/2006RG000197.

Andreadis, K. M., E. A. Clark, D. P. Lettenmaier, and D. E. Alsdorf (2007), Prospects for river discharge and depth estimation through assimilation of swath altimetry into a raster-based hydrodynamics model, *Geophys. Res. Lett.*, *34*, L10403, doi:10.1029/2007GL029721.

Balakrishnan, A. V. (2005), Linear estimation theory, in *Introduction to Random Processes in Engineering*, chap. 9, pp. 359–365, John Wiley, Hoboken, N. J.

Bates, P. D., and A. P. J. De Roo (2000), A simple raster-based model for flood inundation simulation, *J. Hydrol.*, *236*, 54–77.

Burgers, G., P. van Leeuwen, and G. Evensen (1998), Analysis scheme in the ensemble Kalman filter, *Mon. Weather Rev.*, *126*, 1719–1724.

Coe, M. T., M. H. Costa, A. Botta, and C. Birkett (2002), Long-term simulations of discharge and floods in the Amazon Basin, *J. Geophys. Res.*, *107*(D20), 8044, doi:10.1029/2001JD000740.

Dingman, S. (2000), Stream-gaging methods for short-term studies, in *Physical Hydrology*, 2nd ed., Appendix F, pp. 608–622, Prentice Hall, Upper Saddle River, N. J.

Evensen, G. (1994), Sequential data assimilations with a nonlinear quasi-geostrophic model using Monte Carlo methods to forecast error statistics, *J. Geophys. Res.*, *99*(C5), 10,143–10,162.

Frappart, F., S. Calmant, M. Cauhope, F. Seyler, and A. Cazenave (2006), Preliminary results of ENVISAT RA-2-derived water levels validation over the Amazon Basin, *Remote Sens. Environ.*, *100*, 252–265.

Hamilton, S. E., S. J. Sippel, and J. M. Melack (2002), Comparison of inundation patterns among major South American floodplains, *J. Geophys. Res.*, *107*(D20), 8038, doi:10.1029/2000JD000306.

Han, S.-C., C. K. Shum, and A. Braun (2005), High-resolution continental water storage recovery from low-low satellite-to-satellite tracking, *J. Geodyn.*, *39*, 11–28.

Isaaks, E., and R. Srivastava (1989), *Applied Geostatistics*, Oxford Univ. Press, New York.

Melack, J. M., and B. Forsberg (2001), Biogeochemistry of Amazon floodplain lakes and associated wetlands, in *The Biogeochemistry of the Amazon Basin and Its Role in a Changing World*, edited by M. E. McClain, R. L. Victoria, and J. E. Richey, pp. 253–276, Oxford Univ. Press, New York.

National Research Council (2007), *Earth Science and Applications From Space: National Imperatives for the Next Decade and Beyond*, 418 pp., Natl. Acad., Washington, D.C.

Oki, T., and S. Kanae (2006), Global hydrological cycles and world water resources, *Science*, *313*, 1068–1072.

Rodell, M., and J. S. Famiglietti (2001), An analysis of terrestrial water storage variations in Illinois with implications for the Gravity Recovery and Climate Experiment (GRACE), *Water Resour. Res.*, *37*(5), 1327–1339.

Rodríguez, E., and D. Moller (2004), Measuring surface water from space, *Eos Trans. AGU*, *85*(47), Fall Meet. Suppl., Abstract H22C-08.

Smith, L. (1997), Satellite remote sensing of river inundation area, stage, and discharge: A review, *Hydrol. Processes*, *11*, 1427–1439.

Wilson, M., P. Bates, D. Alsdorf, B. Forsberg, M. Horritt, J. Melack, F. Frappart, and J. Famiglietti (2007), Modeling large-scale inundation of Amazonian seasonally flooded wetlands, *Geophys. Res. Lett.*, *34*, L15404, doi:10.1029/2007GL030156.

Wittman, F., W. J. Junk, and M. T. F. Piedade (2004), The várzea forests in Amazonia: Flooding and the highly dynamic geomorphology interact with natural forest succession, *For. Ecol. Manage.*, *196*, 199–212.

D. E. Alsdorf and M. Durand, Byrd Polar Research Center, Ohio State University, 135 E Scott Hall, 109, Carmack Road, Columbus, OH 43210-1808, USA. (durand.8@osu.edu)

K. M. Andreadis and D. P. Lettenmaier, Department of Civil and Environmental Engineering, University of Washington, Seattle, WA 98195, USA.

D. Moller, NASA Jet Propulsion Laboratory, Pasadena, CA 91109, USA.

M. Wilson, Geography, Faculty of Science and Agriculture, University of the West Indies, St. Augustine, Trinidad and Tobago. (matthew.wilson@sta.uwi.edu)